



AIAA 2002-0543

The Role of Formal Experiment Design in Hypersonic Flight System Technology Development

**Charles R. McClinton,
Shelly M. Ferlemann,
Ken E. Rock and
Paul G. Ferlemann**

NASA Langley Research Center, Hampton VA

**40th AIAA Aerospace Sciences
Meeting and Exhibit
January 14-17, 2002/Reno, NV**

The Role of Formal Experiment Design in Hypersonic Flight System Technology Development

Charles R. McClinton, Shelly M. Ferlemann, Ken E. Rock and Paul G. Ferlemann
National Aeronautics and Space Administration, Langley Research Center, Hampton, Virginia 23681-0001

ABSTRACT

Hypersonic airbreathing engine (scramjet) powered vehicles are being considered to replace conventional rocket-powered launch systems. Effective utilization of scramjet engines requires careful integration with the air vehicle. This integration synergistically combines aerodynamic forces with propulsive cycle functions of the engine. Due to the highly integrated nature of the hypersonic vehicle design problem, the large flight envelope, and the large number of design variables, the use of a statistical design approach in design is effective. Modern Design-of-Experiments (MDOE) has been used throughout the Hyper-X program, for both systems analysis and experimental testing. Application of MDOE fall into four categories: experimental testing, studies of unit phenomena, refining engine design, and full vehicle system optimization. The MDOE process also provides analytical models, which are also used to document lessons learned, supplement low-level design tools, and accelerate future studies. This paper will discuss the design considerations for scramjet-powered vehicles, specifics of MDOE utilized for Hyper-X, and present highlights from the use of these MDOE methods within the Hyper-X Program.

INTRODUCTION

Airbreathing launch vehicle research started in the USA in the early 1960's^[1]. The goal, then and now, is to reduce the cost and increase the safety of space access. Current rocket propelled launch vehicles are heavy due to the oxidizer load, and improvement in rocket specific impulse is difficult after years of refinement and optimization. Airbreathing engines capable of operation at or near orbital velocity are proposed to replace rockets^[2]. These engines are based on the supersonic combustion ramjet, or scramjet, engine cycle (figure 1). In theory, the scramjet can operate from supersonic to near orbital velocity.

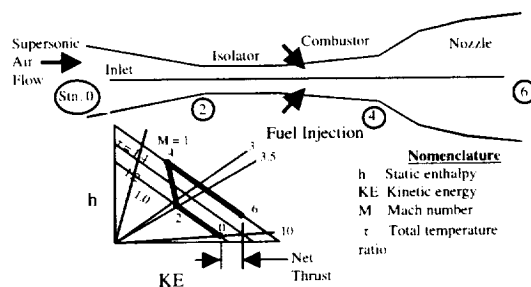


Figure 1. Typical scramjet schematic and thermodynamic Cycle

The scramjet uses a classical Brayton Cycle^[3] to produce power, like both the internal combustion and turbine engines. Air is compressed; fuel injected, mixed and burned to increase the temperature and pressure of the air; then these

combustion products are expanded. For the internal combustion engine, the momentum of the piston provides compression; and the piston, pushed by the high-pressure combustion gas, extracts work. In principle the scramjet works the same. The forward motion of the vehicle compresses the air. Fuel is then injected and burned. Finally, the high-pressure combustion products expand over the nozzle and vehicle aftbody, elevating the surface pressure and pushing the vehicle (rather than the piston). Thrust is the result of increased kinetic energy between the initial (0) and final (6) states of the working fluid.

Specific impulse of airbreathing ramjet, scramjet and turbine engines, compared to the rocket is illustrated in Figure 2. Specific impulse is the thrust produced per pound of propellant utilized per second. For the rocket, propellant includes fuel and oxidizer; for the air breather, only fuel. Note the significant improvement in performance of the air breather vis-à-vis a rocket. For example, the scramjet is 7 times more efficient than the rocket at Mach 7. The dual-mode scramjet operates over the ramjet and scramjet speed range, from about Mach 3 to at least Mach 15. The scramjet is the heart of the hypersonic space access vehicle propulsion system. An airbreathing launch vehicle will require additional propulsion modes, both for high and low-speed operation. Rockets are used at high speed, for orbital insertion, at Mach > 15.

Several options have been studied for takeoff to Mach 3, including turbine, rocket, air-augmented

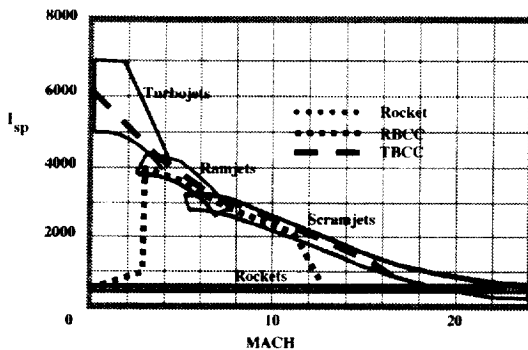


Figure 2. Engine efficiency.

Rocket, ejector ramjet, and pulse detonation engines (PDE). Dashed lines in figure 2 illustrate the efficiency of the turbine-scamjet-rocket combination (TBCC) engine and air augmented rocket – scamjet combined cycle (RBCC) engines currently being developed in the NASA Marshall led Advanced Space Transportation Program (ASTP)^[4].

Early system studies showed that the scramjet must be utilized to high (Mach 14-16) speed^[6] to achieve the airbreathing engine advantage over a rocket. One important and interesting feature in scramjet engine performance is the decreasing specific impulse at higher flight Mach numbers. This is caused by the increasing total enthalpy or kinetic energy of the working fluid; i.e., the air, which is characterized by the “rule of 69”^[5]. The ratio of stoichiometric heat release-to-kinetic energy of the airstream is 69 divided by Mach squared. Thus, at Mach 6, the value is 2, but at Mach 16 it decreases to 1/4. And as a result, thrust becomes a small 10-15% difference between large inlet drag and nozzle thrust, and acceleration becomes the small difference between this thrust and the vehicle drag. Thus achieving the significant benefits of the airbreathing launch system requires effective system development.

Vehicle studies^[7, 8, 9] in the 60’s determined that a hypersonic, airbreathing engine would be too large to mount under a wing. In fact, the engines must be integrated with the vehicle fuselage to capture the large quantities of air required for the engines to accelerate the vehicle. System studies have continued to screen and refine numerous vehicle and engine designs. These systems studies addressed both single stage to orbit (SSTO) and two-stage to orbit (TSTO) concepts

with either rocket based combined cycle (RBCC) or turbine “low-speed” systems.^[10, 11] Significant advancements in vehicle systems and scramjet propulsion were accomplished by the USA’s National Aerospace Plane (NASP^[12]) Program. NASP considered a broad spectrum of configurations^[11] ranging from wing-body to lifting body to conical to inward-turning “funnel” arrangements (see figure 3). The preferred lifting body configuration (figure 4) for the space access mission provides the best balance between engine and vehicle size for an

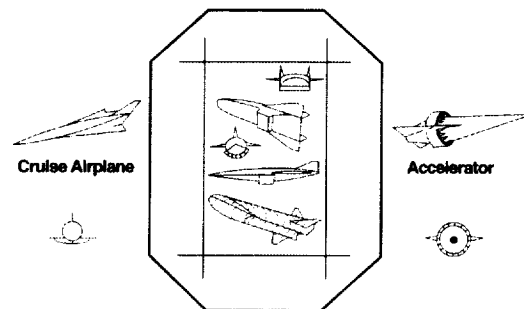


Figure 3. Aerospace Plane Matrix

accelerator. With this configuration, most of the airflow compressed by the forebody is directed into the scramjet inlet. This high air capture is essential for accelerating launch vehicles.

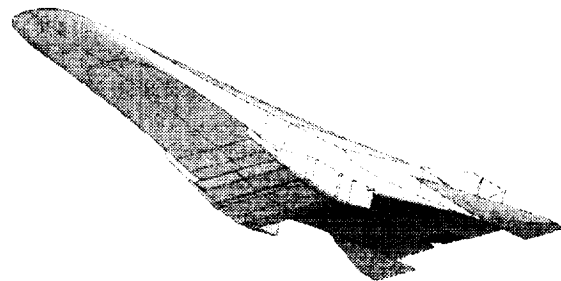


Figure 4. Preferred Lifting Body SSTO Configuration

This paper focuses on design approaches for the scramjet-powered system. While the low-speed engine system is an added complication to the design process, it is not discussed herein.

HYPERSONIC VEHICLE LINES AND DESIGN GUIDELINES

The three-dimensional (3-D) engines on the lifting-body configuration (figure 4) can be represented as two-dimensional (2-D) for system design purposes. Figure 5 illustrates a typical scramjet “flowpath” and vehicle “mold line.” Engine performance is established by solving the

flow field from free stream, through the engine and over the lower vehicle aftbody to resolve the

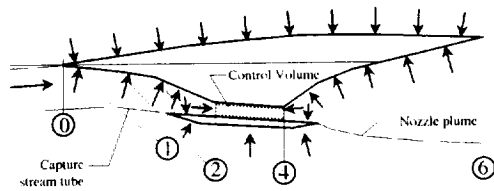


Figure 5. Two-dimensional representation of scramjet powered vehicle.

body forces shown in figure 5. The engine forces and moments are generally reported on the body axis, from the engine cowl leading edge, to vehicle tail. Aerodynamic forces are determined by solving the airflow field around the vehicle, and include the upper surface, vehicle lower forebody, external cowl surface and control surfaces. This 2-D representation of the lifting body vehicle illustrates the designer's challenge to derive a shape which not only provides adequate thrust to drag, but can be efficiently trimmed over a large speed range.

Additional details of the scramjet combustor are shown in figure 6. The combustor is composed of an inlet isolator, high speed fuel injector at the combustor entrance, a constant area or slightly

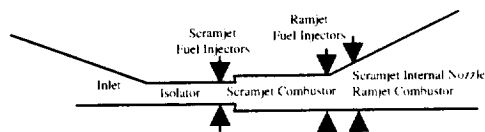


Figure 6. Dual Mode Scramjet Combustor

diverging high-speed scramjet combustor section, and one or two downstream fuel injector stations for ramjet operation. The scramjet internal nozzle doubles as a ramjet combustor. Design guidelines have been developed for inlet contraction ratio, shock strength limits for boundary layer interaction, boundary layer transition, isolator length, fuel injector mixing and drag, combustor area/heat release scheduling, combustor expansion limits, full and reduced rates for finite rate chemical kinetics, base pressure, and nozzle thrust coefficients. These models are utilized in system analysis. Some of these design guidelines/models address operability limits, while others address performance.

Fuel is injected into the combustor from the top (body side) and bottom (cowl) walls at different

combustor area ratio locations (see figure 6). Fuel injection can also be from struts (which distribute the fuel into the air) or bumps (including "ramps") on the wall which help lift the fuel and cause vortices to stir the flow, or by various forms of flush wall injectors. Flush wall injectors have a structural advantage, but produce slower mixing. In stream injectors require cooling, but create faster mixing; potentially reducing engine weight, surface area, and total cooling requirements while increasing thrust.

For these predominantly "2-D" designs, inlet and nozzle design concepts as well as design tools are well characterized. Combustor design tools are less mature and continue to require study to improve mixing and combustion without increasing flow losses or violating structural/material limitations. In addition, integration of the flowpath for efficient operation over a large flight envelope continues to be refined. Engine variable geometry is required, and continued refinement of design concepts is reducing engine weight.

HYPERSONIC VEHICLE DESIGN TOOLS

Airbreathing vehicle systems studies are complex due to the highly integrated nature of the airframe and engine^[13]. Therefore, the vehicle and engine are developed together. A formal design process is illustrated in Fig. 7. Engine and

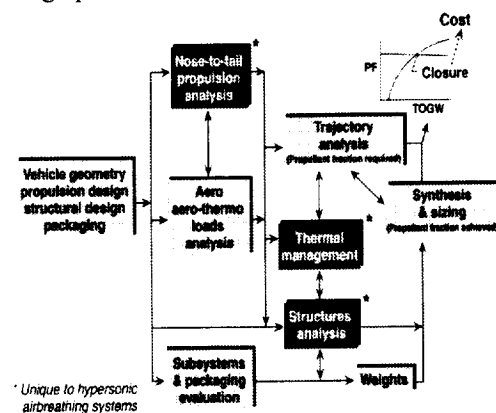


Figure 7. Design Method for Airbreathing Hypersonic Systems.

aerodynamic performance, structure, weight, systems and packaging, and thermal management are iterated as the vehicle is "flown" to determine the "required" propellant volume. Finally, the vehicle is resized to package the propellant required to meet the mission and define a "closed" configuration.

Systems analysis methods for airbreathing vehicles have evolved dramatically over the past 20 years. These methods can be executed at several levels^[10], as noted in Table 1. The efforts discussed herein are performed using level 2 methods: both certified analytical (SRGULL, APAS, etc.)^[11] and CFD based methods.

Level	Color Code	Propulsion	Aero	Structure Weight	Vehicle Performance	Synthesis & Packaging
3	Blue	Flight Data	Flight Data	Flight Vehicle	Flight Vehicle Performance	Flight Vehicle
		Wind Tunnel Data	Wind Tunnel Data	Components Fab/Test	6 DOF Hardware Simulation	Mock-up CAD Multi-Eqn Non-linear
	Green	CFD Certified	CFD Certified	FEM Certified	3 DOF/6 DOF Trimmed	CAD Multi-Eqn Non-linear
2	Light Green	Cycle Certified	Engineering Methods Certified	Unit Loads Certified	3 DOF Trimmed	CAD Multi-Eqn Non-linear
		CFD Uncertified	CFD Uncertified	FEM Uncertified	3 DOF untrimmed	Single Eqn Non-linear
1		Cycle Uncertified	Engineering Methods Uncertified	Unit Loads Uncertified	Energy State	Single Eqn Linear
	Red	Ideal Cycle	UD Cd Estimated	Design Tables	Rocket Equation	Estimated
0						

Table 1. Vehicle Fidelity Assessment.

As noted above, space access vehicle configurations have been baselined. However, because of a relatively low level of maturity of airbreathing vehicle system development, substantial improvements, refinements, and optimization are not only possible but are a significant part of the current development process. The NASA Langley Research Center hypersonic community has attempted several Multiple Disciplinary Optimization approaches. Modern Design-of-Experiment methods have proven extremely useful in refining vehicle and engine design concepts.

MODERN DESIGN-OF-EXPERIMENTS METHODS

Modern Design-of-Experiments (MDOE)^[15,16] studies within the Hyper-X community are used for experimental testing, model development, and to optimize performance of the Hyper-X^[14] and vision^[10] vehicles. The MDOE process was selected because of the large number of independent design variables. By using MDOE, a large number of variables can be investigated efficiently. MDOE uses statistical methods to build polynomial approximate models for the response (component or system performance) to multiple independent design variables. Because of the analytical nature of the parametric model, multiple regression analyses can be used to build and evaluate these models. In addition, the model can either be optimized or studied to determine important design variables.

Modern Design-of-Experiments studies within the Hyper-X community utilize the central composite design^[16] (CCD) approach to define a test or analysis matrix. The CCD technique is a part of response surface methodology^[17] (RSM) by which the relationship between the response (dependent variable) and a set of independent variables can be established. Responses are generated for all points in the test or analysis matrix. For Hyper-X, this is accomplished either by CFD, analytical, experimental, or complete multidisciplinary system analysis (figure 7). Response surfaces are then generated for the individual responses.

Non-linearity and strong two-parameter interactions are expected for both the scramjet and hypersonic vehicle. At least three levels for each of the design parameters are required in order to capture nonlinear effects. Therefore, a second-order model as shown in equation (1) is essential: x_i terms are the design parameters that affect the response variable y , and b 's are regression coefficients. The number of analyses or experiments for the CCD method compared to those for a full factorial design is illustrated in Table 2. The benefit of the CCD approach is apparent for any design with 5 or more independent variables.

$$y = b_0 + \underbrace{\sum_{i=1}^n b_i x_i}_{\text{linear}} + \underbrace{\sum_{i=1}^n b_{ii} x_i^2}_{\text{non-linear}} + \underbrace{\sum_{i=1}^n \sum_{j \neq i}^n b_{ij} x_i x_j}_{\text{two-parameter interaction}} \quad (1)$$

The face-centered CCD technique^[16] was selected because it automatically allows the inclusion of all two-parameter interactions. It also requires 3 levels rather than 5 normally required. This is especially important for a problem with a large number of design parameters, and when the relative significance of the interactions is not known a priori.

The strategy of the CCD method is to statistically select experiment design points (configurations) to acquire a reasonable distribution of data points throughout the design space so that the response can be meaningfully characterized. This design point selection process yields a mathematically well-defined matrix for multiple regression analysis using the least squares method. The JMP^[18] or Design-

Expert^[19] statistical software is used to perform the MDOE point selection. In defining the independent variable the entire system

Number Of Variables	Full Factorial Design	CCD
2	9	9
3	27	15
4	81	25
5	243	27
6	729	45
7	2187	79
8	6587	81
9	19683	147
10	59049	149

Table 2. Design point requirements for 2nd order model.

operability is considered to reduce the potential of points that cannot be resolved. After defining the matrix, the experiment or analysis is performed. Points determined not possible to resolve or responses clearly outside acceptable performance/operability bounds are replaced with closely redefined points, generally with some impact on the variance of the regression coefficients in the CCD matrix. (Significant non-linear operations, like operation on both sides of Mach 1, or with inlet started-to-unstarted, or with combustion and flame blowout should be avoided, unless the study is focused on those phenomena.)

Analysis of the responses is accomplished using a multiple regression analysis. A predictive model, which is the relationship between the responses and two or more independent variables, is developed using the method of least squares. This process is performed using the JMP^[18] or Design-Expert^[19] software, which calculates the coefficients of the regression equation for a second order model. These statistical packages are also utilized to generate Pareto plots^[20], which illustrate the relative influence of the independent variables on the response. In addition, a coefficient of determination is generated by the JMP code, showing how well the regression equation matches the response database.

Finally, the response regression equation can be used to search for an optimum set of independent variables. This is accomplished using various methods: Excel^[21] optimizer; the POST^[22] regression equations; or an in house optimization

code. The in house optimization code was designed to cover the entire parameter database, so as not to be limited to local optimums seen in some Excel solutions.

MDOE APPLICATIONS FOR HYPER-X

The Hyper-X program used MDOE continuously from its inception in 1995. MDOE use falls into four categories:

- Model Development
- Engine Refinement
- Complete Vehicle Refinement
- Experimental Testing

Model development - Numerous analytical or empirical models are required in vehicle design. For "level 0" analysis (Table 1), these include component efficiencies, such as inlet kinetic energy efficiency, isolator pressure rise and total pressure recovery, fuel injector drag, fuel mixing and combustion, wall shear, flow distortion coefficients, nozzle thrust coefficient, aerodynamic forces and moments, and trim forces. For the baseline "Level 2" propulsion design and analysis, the SRGULL^[11] method is used. Correction factors are used for 3-D effects, such as mass spillage, sidewall compression, fuel mixing, and nozzle lateral expansion.

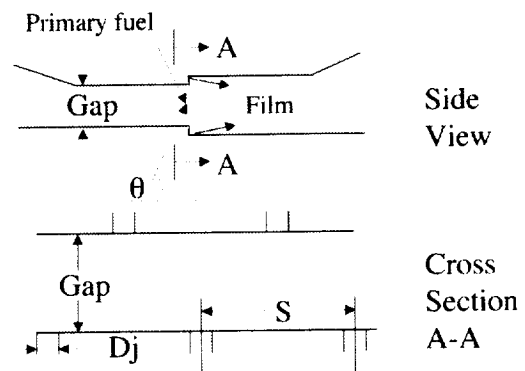


Figure 8. Flush Wall Injector Design Variables.

Mixing was originally defined by the Langley Mixing Recipe^[24]. This model also defines the placement^[24] of normal, sonic hydrogen-fuel flush wall injectors. Figure 8, a cross-section of the combustor at the injector station, illustrates design parameters for placement of the injectors. For the Langley recipe, the opposite wall injectors are inter digitated. Injector lateral spacing on one wall is equal to the combustor height ($S = \text{Gap}$). Fuel mixing efficiency (η_m) for this arrangement is:

$$\eta_m = 1.01 + 0.176 * \ln(x / x_\phi) \quad (2)$$

where -

$$x_\phi = 60 * \text{Gap} * 0.179 e^{(1.72 * \phi)} \quad \text{for } \phi < 1 \quad (2-a)$$

$$x_\phi = 60 * \text{Gap} * 0.333 e^{(-1.204 * \phi)} \quad \text{for } \phi > 1 \quad (2-b)$$

The Langley Mixing Recipe requires 60 gaps for 100% mixing for stoichiometric operation. For non-stoichiometric operation mixing is much faster.

Flush wall injector design was recently investigated using MDOE methods. Independent parameters selected for this study, illustrated in figure 8, are:

- θ Injection angle (0° parallel to wall)
- $P_{t,j}$ Injector total pressure
- ϕ Fuel equivalence ratio
- FS Fuel splits (film total)
- HS Injector spacing to gap, S/Gap
- M Flight Mach number
- Xc Combustor length.

For this MDOE study, all fuel injectors are Mach 2 (rather than sonic, Mach 1, for the LaRC recipe).

A test point matrix was defined for 3-values of the first 6 independent variables. Combustor length was included by post processing the longest combustor solutions. This matrix baseline was the flight vehicle and scramjet for the SSTO configurations shown in figure 4^[10]. This MDOE study used three-dimensional CFD to solve the scramjet combustor reacting flow fields. Forebody and inlet CFD solutions provided initial conditions for the 3-D combustor CFD. A limited number of 2-D nozzle solution were performed, using the combustor solutions for inflow conditions, to characterize the nozzle performance.

Responses documented from the study include:

- η_m Mixing efficiency
- η_c Combustion efficiency
- $P_{t,4}/P_{t,2}$ Combustor total pressure recovery
- C_f Combustor total shear drag
- $q_{w,m}$ Maximum wall heat flux
- Q_w Total heat transfer to wall
- $\eta_{D,1}$ Distortion parameters (mass, momentum and energy)
- C_s Scramjet nozzle discharge coefficient
- M_c Combustor 1-D Mach number
- p_c Combustor static pressure
- $T_{p..}$ Combustor thrust potential
- Δs Combustor entropy

Each of these responses was post processed from individual CFD solution data planes, or

combustor cross-sections, or other CFD output files. Regression equations were developed for these responses, as discussed above.

This MDOE study used combustor thrust potential (T_p)^[3] to identify the flush wall injector design that produced maximum thrust. Thrust potential is cowl to tail engine thrust:

$$T_{p..} = F_6 - F_1 \quad (3)$$

where “F” is stream momentum, and the stations are identified in figures 1 and 6. Engine exit momentum is calculated by expanding individual combustor station conditions to the vehicle trailing edge. Figure 9 illustrates optimized thrust potential (vs. combustor length, in Gap’s) for flight Mach 10, $\phi = 1.0$, and with the best injector design. Characteristic of the “best injector” are listed on the figure. This figure

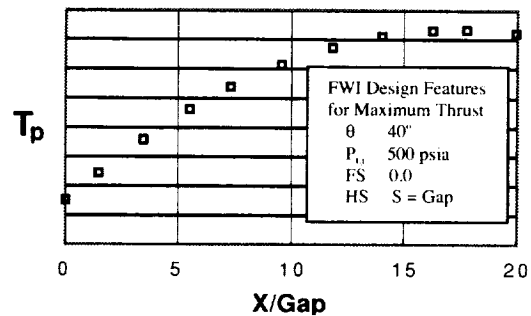


Figure 9. Thrust Potential, Mach 10, $\phi = 1.0$.

demonstrates rapidly increasing T_p in the first 5–10 gap-lengths of the combustor. Then the rate of increase in T_p gradually falls off. In fact, if the engine combustor is extended beyond 15 gaps T_p decreases. This is a result of slow mixing and combustion adding less energy than losses due to shear, heat transfer and subsequent nozzle losses. Excel optimization was designed to search for maximum values of T_p throughout the combustor length, not just at the exit.

The fuel mixing efficiency responses at three combustor lengths were fit with three regression equations. These equations were then fitted by equation 3, to incorporate combustor length into a single regression model:

$$\begin{aligned} \eta_{mix} = & 0.0364 + 0.5668 * FS + 0.249 * HS \\ & + 0.2223 * \Phi + 0.0002026 * \theta \\ & - 0.2973 * M + 0.000011925 * P_{T,j} \\ & + 0.0002031 * \theta * M - 0.3492 * FS * \Phi \\ & - 0.2133 * FS * HS - 0.003980 * FS * \theta \end{aligned}$$

$$\begin{aligned}
& - 0.0857 * HS * \Phi + 1.696 * Xc \\
& - 0.1103 * (Xc^3) - 0.00588 * FS * Xc^2 \\
& - 0.3104 * FS * Xc \\
& - 0.4134 * HS * \exp(-24 * \exp(-2 * Xc)) \\
& + 0.0376 * \Phi * \exp(-20 * \exp(-2 * Xc)) \\
& + 0.06326 * M * ((Xc - 2)^2) \\
& - 0.0003588 * \theta * Xc^2 \\
& + 0.0000395 * P_{TJ} * (Xc - 0.5)^{0.6}
\end{aligned} \quad (4)$$

The corresponding fuel mixing efficiency for the flush wall injector design (figure 9), which produced maximum thrust, is shown in figure 10. Mixing efficiency is about 80% at 16 gaps, the length identified to provide the best thrust. A combustor length of about 35 Gaps is required to achieve 95% mixing. However, a combustor designed to achieve 95% mixing or combustion efficiency would have significantly less thrust. This study illustrates the necessity to design each component considering the entire system, not just component efficiency.

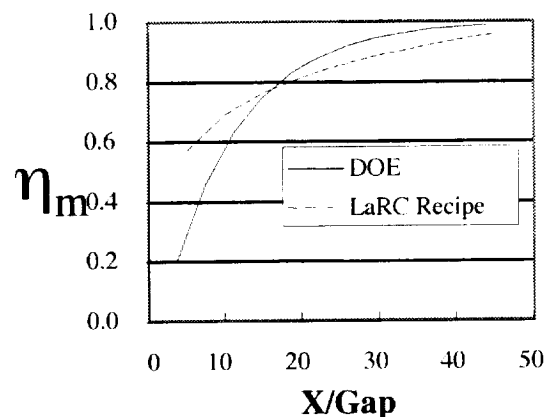


Figure 10. Fuel Mixing efficiency for "best" FWI, Mach 10, $\Phi = 1$.

Figure 10 also presents a comparison of the MDOE and LaRC Mixing Recipe, showing reasonable agreement between the models. In addition, note that the MDOE results confirm the recipe recommended injector spacing of $S = \text{Gap}$.

Validation of the MDOE results was attempted in the Calspan 96" reflected shock tunnel (RST), the LaRC HYPULSE expansion tube at GASL, and the Ames Research Center 16" RST with tests over the speed range $10 < \text{Mach} < 17$. Unfortunately, data quality was inadequate to resolve the performance better than $\pm 20\%$. Tests are continuing with the Hyper-X configuration. Never the less, comparison with high quality non-reacting^[26] data has shown that fuel mixing predictions within 5% are possible.

Engine Refinement – The Hyper-X vehicle (figure 11) is a 6% scale version of a Mach 10 cruise, Dual-Fuel, Global-Reach (DFGR) vehicle^[25]. The original Hyper-X vehicle/engine keel line corresponded to a photographically scaled version of the DFGR vehicle variable geometry design at Mach 7 and 10. Because of physical scale and viscous and finite rate chemical kinetic effects^[5], changes to the engine flowpath at both Mach 7 and 10 were required to achieve acceleration. This discussion addresses the difficult Mach 10 flight condition.

Vehicle acceleration for the Mach 10 X-43 flight vehicle remained inadequate after the first refinement study. In addition, thermal loads required excessive active cooling. A two-cycle MDOE approach was then used for the engine refinements required to meet the program objectives for the Mach 10 design:

- Assured measurable acceleration (acceleration greater than uncertainty)
- No active cooling except Mach 7 engine leading edge design/flow rates
- Operability (with margin)
- Mach 7 vehicle outer mold line.

The outer loop addressed gross features of the engine, and the inner loop focused on combustor details.

The outer loop considered 9 design parameters: these included 2 flight conditions (Mach number and angle of attack), 3 inlet parameters, 3 combustor parameters, and 1 nozzle parameter.

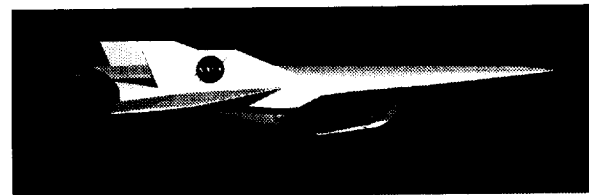


Figure 11. Hyper-X Mach 10 Research Vehicle.

Inlet parameters included contraction ratio, inlet cowl length and internal contraction angles. Combustor parameters addressed combustor length and area ratio. Finally, the one nozzle parameter was initial expansion angle. The outer loop MDOE was performed using the SRGULL^[11,13] code with 3-D flow field corrections, one-dimensional finite rate chemistry, and the Hyper-X vehicle aerodynamic database. Three-dimensional corrections included forebody mass spillage, sidewall compression and shear, 3-D fuel mixing

model (like equation 4), and 3-D nozzle expansion effects. (It should be noted that this study included 16 variables — 7 of which were eliminated by analysis of two screening matrices).

Twenty-nine responses were tracked for the outer loop, SRGULL matrix. This large number was selected to include parameters that may be required in the future, in addition to parameters of interest in this optimization study. An optimization tool developed for this study varied each design variable independently, and an optimized design found based on trimmed net axial force. This optimization was originally run unconstrained. As other design guidelines were identified and incorporated a new optimum configuration was identified. Some of these constraints were identified by the inner loop matrix analysis. The new engine flow lines generated by this outer loop MDOE study formed the baseline for the inner loop analysis.

The inner loop design was limited to 5 variables due to the increase from 27 to 45 case solution matrices required for an increase from 5 to 6 variables (table 2). The variables selected included fuel injector details similar to those discussed regarding figure 8. The inner loop also included inlet contraction ratio because of the potential to change when combining results from both inner and outer loop analysis.

The analysis matrix for the MDOE study included 27 cases for the 5 variables and 3-levels. 3-D CFD was used to resolve these combustor designs. Inflow for the solutions was provided by 2-D CFD solutions of the forebody and inlet. Each combustor solution was continued through the nozzle to determine the nozzle performance.

As with the outer loop, trimmed vehicle axial force was used as the primary response. Other responses (20) were used to check operability limits — like a thermal load parameter for the combustor. Results from the inner loop analysis were combined with the outer loop to define a refined configuration, designated keel line 6 (KL-6). This design was predicted to have a 25% increase in engine thrust, which met program goals.

Verification of the design was accomplished by experiments in the HYPULSE and LENS reflected shock tunnels. Small changes were made to the constraints after the first test in HYPULSE, and a new configuration (KL-8) was

identified using the MDOE database, and verified in subsequent tests.

Full vehicle refinement –

The Hyper-X Program also used Modern Design-of-Experiments to refine complete space access vehicle concepts. Ferlemann^[21] demonstrated the approach and method on a simple configuration. The Turbine scramjet combination (TBCC) Air Breathing Launch Vehicles, figure 12^[10], was optimized over the Mach 4 to 15 scramjet and “LOX addition” Mach 15-22 operating ranges using the vehicle level methods discussed in reference 23. This study used 15 independent design variables. These design variables include flight conditions, vehicle shape, as well as engine location and geometry. The “Design-Expert” code was utilized to identify the solution points for the analysis matrix. These conditions are passed to the

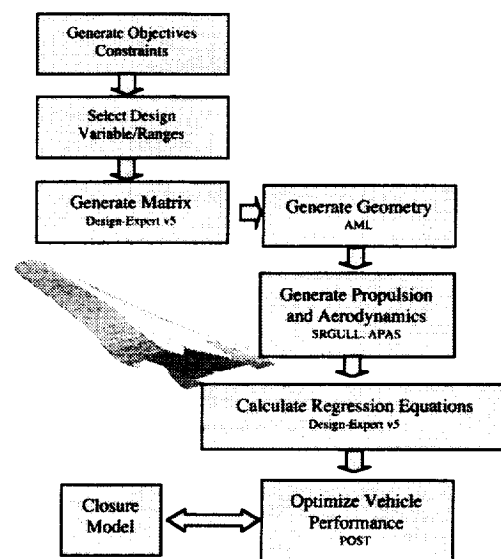


Figure 12. LaRC automated MDOE ABLV Design Process.

AML code, which provides automated geometry definition (file) for the propulsion and aerodynamic analysis. The SRGULL code was used to solve the design matrix propulsion, and APAS the vehicle aerodynamics. The SRGULL solutions are performed, utilizing numerous 3-D models, as discussed above. (Other design disciplines, shown in figure 7, are being brought into this optimization process.) Forty-one (41) output responses were tracked. Regression equations for these response surfaces were generated using the “Design-Expert” code. Propulsion and vehicle performance and

operability regressions are input into the trajectory optimization code POST, along with mass properties, mission requirements and trajectory/operational constraints. The POST code is then used to find a solution, and proceeds to optimize the vehicle and flight trajectory to minimize vehicle TOGW (see ref. 23 for additional details on this process). The design process is illustrated in figure 12.

Regression models developed in this process add to the design database for future trade studies.

These MDOE analyses have identified ways to reduce the launch vehicle take off gross weight, while adding to the configurations fidelity. The 25,000-pound payload to International Space Station (ISS) requirement^[2] for NASA's Advanced Space Transportation Program can be achieved using a hypersonic airbreathing vehicle, either with turbine low speed system (TBCC) or with RBCC. These SSTD vehicles have takeoff gross weight of 1.0 million pounds and 1.6 million pounds respectively.

Two other vehicle level applications of MDOE have been completed: One of these is conceptual design of a government baseline X-43B RBCC flight demonstrator vehicle^[12], shown in figure 13.

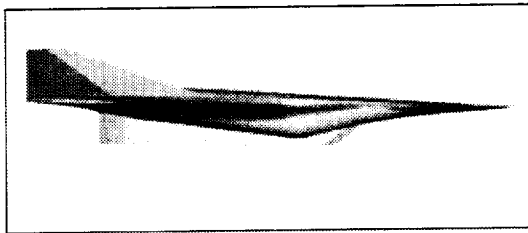


Figure 13. X-43B RBCC Vehicle Design.

SUMMARY

Hypersonic airbreathing vehicles offer large gains in propulsive efficiency over rockets. Unlike rocket powered vehicles, scramjet powered hypersonic vehicles require a high degree of optimization, due to large flight envelope and reduced thrust to weight and drag. Scramjet powered vehicle design incorporates a huge number of variables, including some linear and non-linear effects, and unknown interactions. Hypersonic vehicle design is an ideal problem for multidisciplinary design methods. Design of experiment methods meets these requirements. The Modern Design-of-Experiment (MDOE) method is used in the Hyper-X program, for

guiding both systems analysis and experimental testing. Face-centered, central composite design was utilized in most applications, to define a matrix of point for test or analysis. Responses, generated by test or analysis, are analytically defined relative to the design variables using least squares multiple regression analysis. Regression equations are used to model the responses, search for an optimum, and document sensitivities.

MDOE use in Hyper-X falls into four categories: Experimental Testing, Model Development, Engine Refinement, and Complete Vehicle Refinement. For model development, MDOE solutions have provided significant advancement over previous models, such as fuel mixing models. MDOE application to the Mach 10 X-43 flight scramjet redesign provided a 25% increase in engine thrust, meeting program goals and schedule. MDOE methods are being automated for application on a complete vehicle.

ACKNOWLEDGEMENTS

Special thanks go to Mr. Steven Beckel, P&W Space Propulsion for introducing multidisciplinary design methods to the scramjet community.

REFERENCES

1. Heiser, W.H. and Pratt, D.T.: Hypersonic Airbreathing Propulsion. AIAA Education Series. AIAA, Inc. Washington, D.C., USA. 1994.
2. Hueter, Uwe: Rocket-Based Combined-Cycle Propulsion Technology for Access-to-Space Applications. AIAA 99-4925. Presented at 9th International Space Planes and Hypersonic Systems and Technologies Conference, Norfolk, USA. Nov. 1-5, 1999.
3. Riggins, D.W.; McClinton, C.R.; and Vitt, P.H.: Thrust Losses in Hypersonic Engines, AIAA Journal of Propulsion and Power, Vol. 13, No. 2, pp. 281-295, 1997.
4. Kumar, A.; Drummond, J.P.; McClinton, C.R.; and Hunt, J.L.: Research in Hypersonic Airbreathing Propulsion at the NASA Langley Research Center, Paper 2001-1071, XV ISABE, September 2001.
5. Anderson, G.Y.; McClinton, C.R.; and Weidner, J.P.: Scramjet Performance. Chapter 6. Scramjet Propulsion. AIAA Progress in Astronautics and Astronautics, Vol. 189, 2000.

6. Escher, W.J.D.: Synerjet for Earth/Orbit Propulsion: Revisiting the 1966 NASA/ Marquardt Composite (Airbreathing/ Rocket) Propulsion Study. SAE Progress in Technology Series, PT-54, Chapter 3: The "Synerjet Engine."
7. Douglas Aircraft Company: Two-Stage Aerospace Plane Study. DAC-47551, 1964.
8. Republic Aviation Corp.: Reports related to Single Stage to Orbit Studies. RAC #430, #730 and #1306, 1961-62.
9. Republic Aviation Corp.: Reports related to Two-Stage Aerospace Plane Study. RAC #1370-20-I, Jan. 28, 1964.
10. McClinton, C.R.; Hunt, J.L.; Ricketts, R.H.; Reukauf, P.; and Peddie, C.L.: Airbreathing Hypersonic Technology Vision Vehicles and Development Dreams. AIAA Paper No. 99-4978, November 1999.
11. Hunt, J.L. and Martin, J.G.: Rudiments and Methodology for Design and Analysis of Hypersonic Air-Breathing Vehicles. Chapter 15. Scramjet Propulsion. AIAA Progress in Astronautics and Astronautics, Vol. 189, 2000.
12. McClinton, C.R.; Andrews, E.H.; and Hunt, J.L.: Engine Development for Space Access: Past, Present, and Future. ISABE 2001-1074, September 2001.
13. Hunt, J.L. and McClinton, C. R.: Scramjet Engine/Airframe Integration Methodology. AGARD-CP-600, Vol. 3: Sustained Hypersonic Flight, Paper C-35, 1997.
14. McClinton, C.R. and Volland, R.T.: Hyper-X Program Status. ISABE 2001-1071, September 2001.
15. Hicks, C.R.: "Fundamental Concepts in the Design of Experiments," John Wiley and Son, New York, 1982.
16. Montgomery, D.C.: "Design and Analysis of Experiments," John Wiley and Son, New York, 1991.
17. Box, G.E.P. and Draper, N.R.: Empirical Model-Building and Response Surfaces. John Wiley and Son, New York, 1987.
18. SAS Institute Inc., Cary, NC. JMP, Statistical Discovery Software, Ver. 3.1, 1995.
19. Stat-Ease, Inc.: Design-Expert Software, Version 5.0. Minneapolis, MN, 1999.
20. Wadsworth, H.M.: "Modern Methods for Quality Control and Improvement," John Wiley and Son, New York, 1986.
21. Microsoft Corporation, Cambridge, MA. "Microsoft Excel, Version 5.0," 1994.
22. Powell, R.W. et. Al.: "Program to Optimize Simulated Trajectories (POST)," Version 1.03, Feb. 1998.
23. Ferlemann, S.M.; Robinson, J.S.; Martin, J.G.; Leonard, C.P.; Taylor, L.W.; and Kamhawi, H.: Developing Conceptual Hypersonic Airbreathing Engines Using Design of Experiments Methods. AIAA 2000-2694.
24. Anderson, G.Y. and Rogers, R.C.: A Comparison of Experimental Supersonic Combustor Performance with an Empirical Correlation of Non Reactive Mixing Results. NASA TM X-2429, Oct. 1971.
25. Hunt, J.L. and Eiswirth, E.A.: Dual-Fuel Airbreathing Hypersonic Vehicle Study. AIAA 96-4591, Nov. 1996.
26. Mao, M.; Riggins, D.W.; and McClinton, C.R.: "Numerical Simulation of Transverse Fuel Injection," NASA Conference Publication 10045 for Symposium on Computational Fluid Dynamics in Aeropropulsion, April 1990.
27. Moses, P.L.; Bouchard, K.A.; Vause, R.F.; Taylor, L.W.; Ferlemann, S.M.; Leonard, C.P.; Robinson, J.S.; Martin, J.G.; Petley, D.H. and Hunt, J.L.: An Airbreathing Launch Vehicle Design with Turbine-Based Low-Speed Propulsion and Dual-Mode Scramjet High-Speed Propulsion. 9th International Space Planes and Hypersonic Systems Conference. AIAA-99-4948.

